Beyond Absorption Maxima: The Impact of Wavelength-Resolved Photochemistry on Materials Science

Quinten Thijssen,[a,b] Joshua A. Carroll,[a] Florian Feist,[c] Andreas Beil,[d] Hansjörg Grützmacher,[d] Martin Wegener,[c] Sandra Van Vlierberghe,[b] Christopher Barner-Kowollik*[a,c]

[a.] *School of Chemistry and Physics, Queensland University of Technology (QUT), 2 George Street, Brisbane, QLD 4000, Australia, christopher.barnerkowollik@qut.edu.au*
[b.] *Department of Organic and Macromolecular Chemistry, Polymer Chemistry and Biomaterials Group, Centre of Macromolecular Chemistry, Ghent University, Krijgslaan 281, 9000, Belgium*
[c.] *Institute of Nanotechnology (INT) and Institute of Applied Physics (APH), Karlsruhe Institute of Technology (KIT), Herrmann-von-Helmholtz-Platz 1, 76344 Eggenstein-Leopoldshafen, Germany, christopher.barner-kowollik@kit.edu*
[d.] *Department of Chemistry and Applied Biosciences, ETH Zürich, Vladimir-Prelog-Weg 1, 8093 Zürich, Switzerland*

Table of Contents

1. Supporting information related to the examples provided in the text

Example 1. calculations for the PMMA-based photoresist design

A. Calculation of the molar concentration of ^{Mes}BAPO-NH_2

Given data: a concentration of 0.5 wt.%, a molar mass of 357 g.mol^{-1}, a density of 1 g/cm^{-3}.

$$Molar\ concentration\ (\mathrm{M}) = \frac{0.5\ \mathrm{g}\ x\ 10\ \mathrm{mL.\,g^{-1}}}{357\ \mathrm{g.\,mol^{-1}}} = 0.014\mathrm{M}$$

B. Calculation of absorption coefficient when 99% of the incident light is absorbed after a penetration depth (d) of 2 m

$$I = I_0\, e^{-\alpha d}$$

$$\frac{I}{I_0} = 0.01 = e^{-\alpha d}$$

$$\ln 0.01 = -\alpha d$$

$$\alpha = -\frac{\ln 0.01}{d} = 0.023\ \mathrm{cm^{-1}}$$

C. Calculation of the molar absorption coefficient

$$\alpha_{abs} = \varepsilon_{abs}\, c\, \ln 10$$

$$\varepsilon_{abs} = \frac{\alpha_{abs}}{c \ln 10} = 0.713\ \mathrm{L\ mol^{-1} cm^{-1}}$$

D. Calculation of the penetration depth at which 99% of the light is absorbed in case of a molar absorption coefficient of 341 L mol^{-1} cm^{-1} (λ_{385})

$$\alpha_{abs} = \varepsilon_{abs}\, c\, \ln 10 = 11.007\ \mathrm{cm^{-1}}$$

$$d = -\frac{\ln 0.01}{11.007} = 0.418\ \mathrm{cm}$$

Example 2. Photoresist based on photo-dimerization of styrylpyrene

A. Calculation of absorption coefficient when 99% of the incident light is absorbed after a penetration depth (d) of 2 m

$$I = I_0\, e^{-\alpha d}$$

$$\frac{I}{I_0} = 0.01 = e^{-\alpha d}$$

$$\ln 0.01 = -\alpha d$$

$$\alpha = -\frac{\ln 0.01}{d} = 0.023\ \mathrm{cm^{-1}}$$

B. Calculation of the chromophore concentration (c)

Molar absorption coefficient (ε) at 450 nm: 85 L mol^{-1} cm^{-1}

$$\alpha_{abs} = \varepsilon_{abs}\, c\, \ln 10$$

$$c = \frac{\alpha_{abs}}{\varepsilon_{abs} \ln 10} = 1.175\ x\ 10^{-4}\ \mathrm{mol\ L^{-1}}$$

C. Determination of the structure and molar mass of suitable end-functionalized precursor

$$M_{chromophore} = \frac{1}{1.2\ x\ 10^{-4}\ \text{mol L}^{-1}} = 8510\ \text{g mol}^{-1}$$

$$M_{tri-functional} = 3\ x\ 8519\ \text{g mol}^{-1} \cong 25\ 000\ \text{g mol}^{-1}$$

2. Supporting information related to the reported figures

Figure 1. normalized number of photons as a function of penetration depth

The intensity I(d) of light at a depth d in a medium is given by the Beer-Lambert's law:

$$I(d) = I_0 . e^{-\alpha d}$$

Here, *I*(d) is the light intensity at depth *d*, I_0 is the initial light intensity at depth = 0, α is the absorption coefficient of the medium. The normalized number of photons at depth *d*, denoted as *N*(*d*), is the ratio of the intensity at depth d to the initial intensity I_0:

$$N(d) = \frac{I(d)}{I_0} = \frac{I_0 . e^{-\alpha d}}{I_0} = e^{-\alpha d}$$

Therefore, the normalized number of photons N(d) is directly related to the intensity I(d) by the expression:

$$N(d) = \frac{I(d)}{I_0}$$

This relationship shows that the normalized number of photons at any depth is simply the intensity at that depth divided by the initial intensity, providing a dimensionless measure that facilitates comparison across different conditions.

Figure 4. Calculation of the intensity profile as a function of vial radius in tomographic volumetric 3D printing

To illustrate the light intensity profile across a cylindrical vial that is rotated and irradiated from outside, we used a computational approach based on the Lambert-Beer law. We created a two-dimensional grid representing the vial's top view, calculating the radial distance R from the center of the vial using $R = \sqrt{X^2 + Y^2}$

The light intensity I at each point within the vial was calculated using:

$$I = I_0\ e^{-\alpha(r_0 - R)}$$

3. Supporting information related to the photochemical action plot of the photopolymerization of PMMA using ^{Mes}BAPO-NH$_2$ as photo-initiator

3.1 Chemicals, synthetic considerations and analytical methods

Methylmethacrylate (MMA, Sigma-Aldich, 99 % stabilized) was freed from the inhibitor by passing through a column of activated basic (Brockmann I) alumina (Sigma-Adlrich).

Reagents and solvents for BAPO synthesis have been purchased from commercial suppliers or obtained from companies as gifts. All syntheses and manipulation of light sensitive compounds have been performed under the exclusion of light. Manipulations of air sensitive materials have been performed under argon in a glovebox (M. Braun) or using standard Schlenk technique. Dry solvents have been degassed with argon and purified using a solvent purification system (Pure solv), purchased from commercial suppliers or distilled from appropriate drying agents. If the terms “dry solvents”, “inert conditions”, or “under argon” are mentioned, oven dried glassware was used under Schlenk technique or in a glovebox.

NMR spectra have been recorded on a Bruker Avance 500 MHz spectrometers. Chemical shifts are reported in ppm relative to $SiMe_4$ (for ^1H and ^{13}C) and 85 % phosphoric acid (for ^{31}P) using the solvent deuterium signals as internal standards. FT-IR spectra have been recorded on a Bruker Tensor II IR spectrometer with Pike MIRacle ATR unit. Opus 7.5 software has been used for data analysis. Elemental analyses have been carried out at the ETH Zürich Mikrolabor. Single crystal X-ray diffraction measurements were performed on a Bruker Smart Apex, Smart Apex 2, or Venture system. Refinement against full matrix (versus F^2) was obtained with SHELXT (Version 6.12) and SHELXL-97 using Olex2.[1]

3.2 Synthesis and characterization of ^{Mes}BAPO-NH$_2$

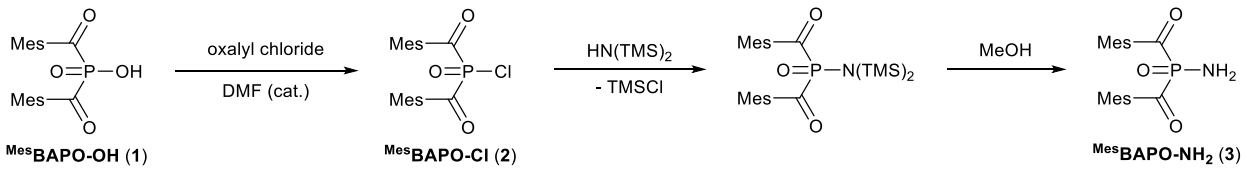

Figure S1. Overview of the synthetic pathway and intermediated reaction products.

Bismesitoylphosphinic acid ^{Mes}BAPO-OH (**1**), synthesized according to an established procedure,[2] is dissolved in THF (ca. 2 mL per mmol) under inert conditions and dry dimethylformamide (ca. 0.12 eq.) is added as nucleophilic catalyst. Upon the dropwise addition of oxalyl chloride (1.5 eq.), a strong gas evolution is observed. After stirring the reaction mixture for 2 h at r.t., all volatiles including excess reagent and catalyst are removed in vacuo overnight. Crude bismesitoylphosphinic chloride ^{Mes}BAPO-Cl (**2**) is obtained as orange solid and used for subsequent syntheses without further purification. ^{Mes}BAPO-Cl (**2**) is prepared from ^{Mes}BAPO-OH (**1**) (54.5 g, 152 mmol) according to the abovementioned procedure and mixed with 400 mL of dry THF yielding a yellow suspension. Hexamethyldisilazane

(80 mL, 0.38 mol, 2.5 eq.) is added and the reaction mixture is stirred at 60 C for 6 h. After 5 h, more hexamethyldisilazane (16 mL, 77 mmol, 0.5 eq.) is added. After stirring the reaction mixture for 18 h at r.t., it is cooled in an ice bath and dry MeOH (50 mL, 1.2 mol, 8 eq.) is added to solvolyse BAPO-N(TMS)$_2$. From the obtained yellow mixture, a colourless solid is removed by filtration over a G4 frit yielding a yellow solution, which is evaporated *in vacuo*. The obtained solid is recrystallized from dry DCM (250 mL, boiling temperature to -30 C). An off-white solid is obtained, which is collected by filtration, washed with ca. 20 mL of dry DCM and dried *in vacuo* (30.1 g, 84.2 mmol, 55%). (**3**) is obtained from a DCM solution layered with hexane as colourless crystals suitable for single crystal XRD.

^{1}H NMR (500 MHz, $CDCl_3$, 298 K) δ/ppm = 6.86 (s, 4H, Mes-H), 3.39 (bs, 2H, NH_2), 2.29 (s, 18H, o,p-Mes-CH_3); $^{13}C\{^{1}H\}$ NMR (100.6 MHz, $CDCl_3$, 298 K) δ = 216.9 (d, J_{PC} = 85.6 Hz, PCO), 141.0 (p-Mes), 135.6 (d, J_{PC} = 44.6 Hz, ipso-Mes), 135.6 (o-Mes), 129.1 (m-Mes), 21.2 (p-Mes-CH_3), 19.7 (o-Mes-CH_3); ^{31}P NMR (121.5 MHz, $CDCl_3$, 298 K) δ/ppm = 0.0 (s); FT-IR ν/cm^{-1} = 3393 m, 3236 w, 2978 w, 2951 w, 2918 w, 1669 m, 1644 m, 1606 m, 1548 m, 1454 w, 1441 w, 1424 m, 1377 m, 1295 w, 1248 w, 1226 m, 1215 m, 1192 s, 1153 w, 1145 m, 1030 m, 983 m, 965 w, 941 w, 929 w, 917 m, 884 w, 869 m, 847 s, 731 m, 688 m, 672 m, 622 w; EA (calc.) 67.22 % C, 6.77 % H, 3.92 % N; EA (meas.) 66.76 % C, 6.80 % H, 3.83 % N; UV Vis (THF) λ/nm = 269, 358, 371, 388 (sh).

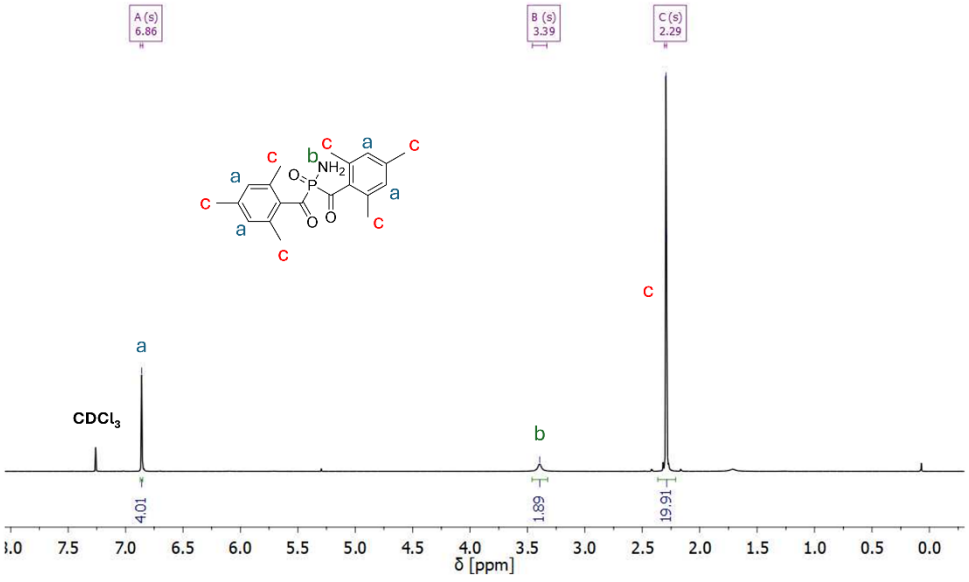

Figure S2. Assigned ^{1}H-NMR spectrum of ^{Mes}BAPO-NH_2.

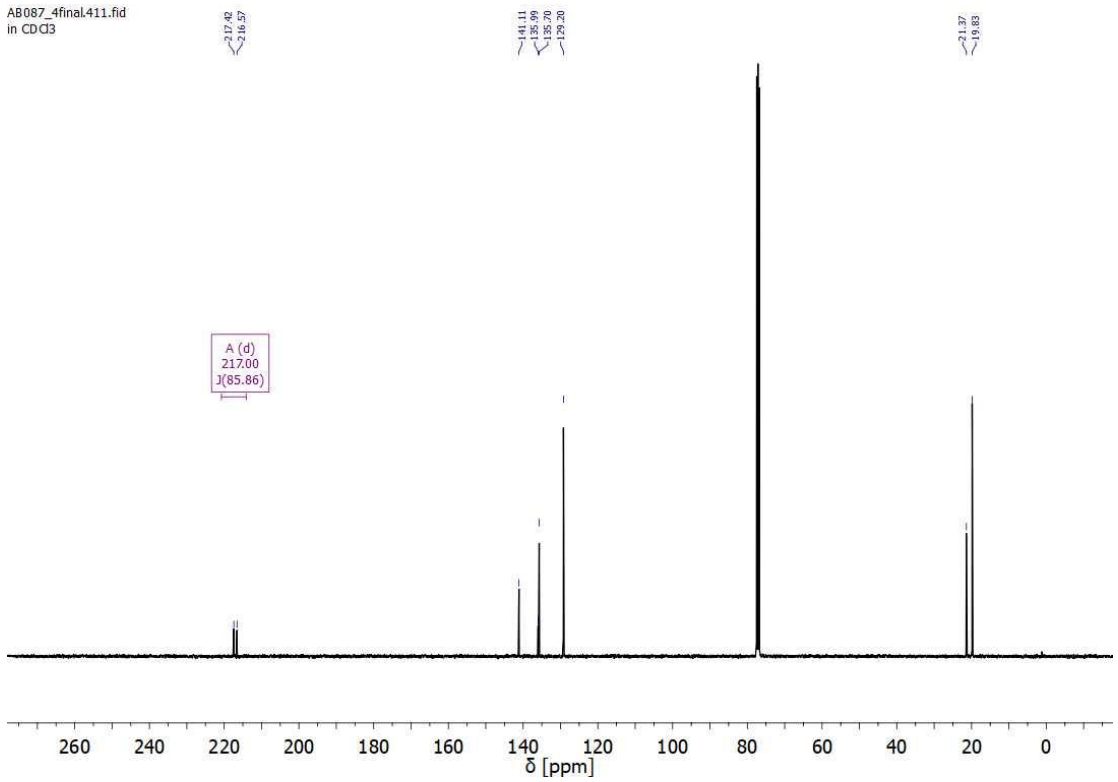

Figure S3. ^{13}C-NMR spectrum of ^{Mes}BAPO-NH$_2$.

3.3 Crystallographic data and ORTEP plots of ^{Mes}BAPO-NH$_2$ and ^{Mes}BAPO-Cl

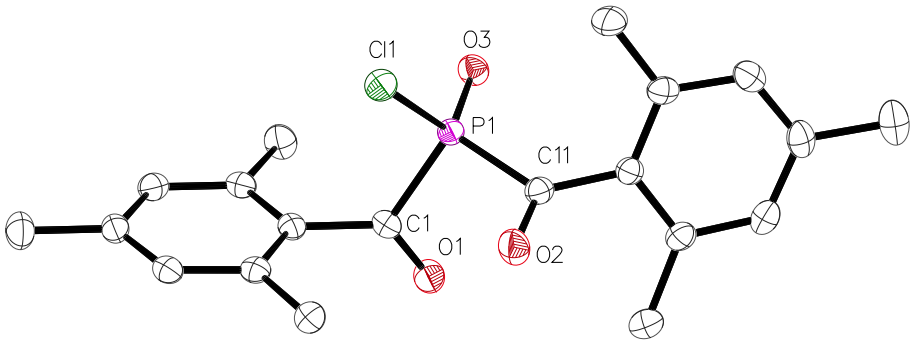

Figure S4. Molecular structure of ^{Mes}BAPO-Cl. For clarity, hydrogen atoms are omitted.

Table S1. Crystal data and structure refinement for ^{Mes}BAPO-NH$_2$ (3) with CSD-2357232

Empirical formula	$C_{20}H_{24}NO_3P$
Formula weight	357.37
Temperature/K	100
Crystal system	monoclinic
Space group	$P2_1/n$
a/Å	12.3856(2)
b/Å	8.80280(10)

c/Å	17.3712(3)
α/°	90
β/°	105.0240(9)
γ/°	90
Volume/Å^3	1829.21(5)
Z	4
ρ_{calc}g/cm^3	1.298
μ/mm^{-1}	0.169
F(000)	760.0
Crystal size/mm^3	0.369 × 0.248 × 0.18
Radiation	MoKα (λ = 0.71073)
2Θ range for data collection/°	3.634 to 55.008
Index ranges	-16 ≤ h ≤ 16, -11 ≤ k ≤ 11, -22 ≤ l ≤ 16
Reflections collected	18311
Independent reflections	4201 [R_{int} = 0.0445, R_{sigma} = 0.0434]
Data/restraints/parameters	4201/0/240
Goodness-of-fit on F^2	1.054
Final R indexes [I>=2σ (I)]	R_1 = 0.0396, wR_2 = 0.0887
Final R indexes [all data]	R_1 = 0.0553, wR_2 = 0.0968
Largest diff. peak/hole / e Å^{-3}	0.31/-0.39

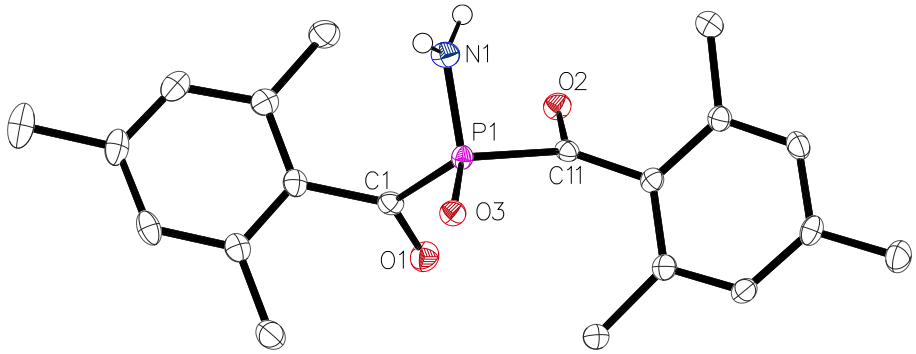

Figure S5. Molecular structure of ^{Mes}BAPO-NH$_2$. For clarity, selected hydrogen atoms are omitted.

Table S2. Crystal data and structure refinement for ^{Mes}BAPO-Cl (2) with CSD-2357233

Empirical formula	$C_{20}H_{22}ClO_3P$
Formula weight	376.79
Temperature/K	100.0
Crystal system	orthorhombic
Space group	$Pca2_1$
a/Å	16.2099(10)
b/Å	16.3341(9)
c/Å	7.1962(4)
α/°	90

β/°	90
γ/°	90
Volume/Å^3	1905.37(19)
Z	4
ρ_{calc}g/cm^3	1.314
μ/mm^{-1}	0.300
F(000)	792.0
Crystal size/mm^3	0.4 × 0.2 × 0.08
Radiation	MoKα (λ = 0.71073)
2Θ range for data collection/°	4.988 to 59.144
Index ranges	-22 ≤ h ≤ 22, -18 ≤ k ≤ 22, -9 ≤ l ≤ 9
Reflections collected	57780
Independent reflections	5310 [R_{int} = 0.0540, R_{sigma} = 0.0270]
Data/restraints/parameters	5310/1/232
Goodness-of-fit on F^2	1.093
Final R indexes [I>=2σ (I)]	R_1 = 0.0382, wR_2 = 0.0827
Final R indexes [all data]	R_1 = 0.0477, wR_2 = 0.0873
Largest diff. peak/hole / e Å^{-3}	0.43/-0.22

3.4 UV-Vis Measurements

UV-Vis spectra of ^{Mes}BAPO-NH$_2$ were recorded on a Shimadzu UV-2700 spectrophotometer equipped with a CPS-100 electronic temperature control cell positioner. Samples were prepared in deinhibited MMA and measured in Hellma Analytics quartz high precision cell cuvettes (d = 10 mm) at 20 °C. To obtain precise values for the extinction coefficient, ^{Mes}BAPO-NH$_2$ was measured at 9 different concentrations and combined considering the upper and lower detection limit of the photospectrometer.

3.5 Tunable laser PLP-experiments with a constant photon count

Tunable laser experiments with a constant photon count at varied wavelengths were carried out according to a procedure that was published earlier:[3–5]

An Innolas Tunable Laser System SpitLight 600 OPO was applied as light source. An optical parametric oscillator (OPO) was pumped with a diode pumped Nd:YAG laser (repetition rate 100Hz). The energy of the laser pulses was downregulated by an attenuator (polarizer). The beam is redirected into the vertical cylindrical hole of a custom-made sample holder, which contains the samples during the experiments (refer to **Figure S6**). These glass vials are crimped 0.7 mL vials by LLG Labware, Lab Logistic Group GmbH (Art. Nr. 4-008202). The energy of the incident laser pulses was measured by an Energy Max PC power meter (Coherent) directly above the sample holder. Prism and sample holder are positioned in a way that the complete diameter of the hole of the sample holder is covered by the incident laser beam. Adapted from previous publications.[3–5]

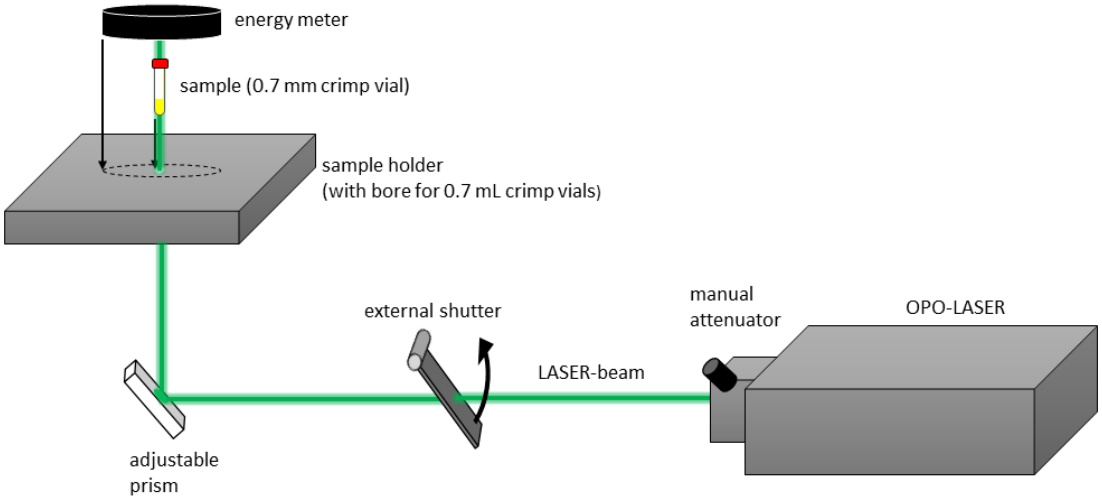

Figure S6. Experimental setup for tuneable laser experiments. The energy output is regulated with the attenuator and controlled with the energy meter (setup without sample). Measurement of energy and irradiation of samples cannot be done simultaneously. An individual setting of the attenuator is necessary before each irradiation experiment. Adapted from previous publications.[3–5]

3.6 Control over the incident number of photons in a tunable laser experiment

The number of photons n_p ([n_p] = mol) that a monochromatic laser pulse contains can be calculated by application of the Planck-Einstein relation from the energy of the pulse E_{pulse}, the incident wavelength λ, Planck's constant h and the speed of light c.

$$n_p = \frac{E_{pulse}\ \lambda}{h\ \ c\ \ N_A}$$

If the absorption of the glass vial and the extent of reflection and scattering at the vial at the respectively relevant wavelength is known, a target energy value can be calculated that must be reached during the above described measurement to guarantee that the desired number of photons penetrates the sample solution during the subsequent irradiation. The wavelength dependent transmittance of the glass vials was determined experimentally using the above setup. Three glass vials were randomly selected as calibration vials. For varying wavelengths and in each case at a constant power output of the laser the energy was measured both with and without the calibration vials fitted into the sample holder.

The measured energy per pulse without a calibration vial in the sample holder is denoted as E_0 and the measured energy per pulse with a calibration vial in the sample holder as E_n. The transmittance was calculated as the ratio of E_n to E_0. The average transmittance over the measurements of the three vials (T_λ) was plotted together with the respective error.

$$T_\lambda = \frac{E_n}{E_0}$$

An analytical fit of a function to the data was not done due to the unexpected deviations of several values from a smooth curve form. It is known that conventional glass can exhibit minor impurities and additives that change the transmittance spectrum for certain wavelengths. The method that is reported here for the determination of the transmittance was chosen, because the exact same setup was used during the photoreactions.

The target energy per pulse E_0 can be calculated directly from the wavelength λ, the number of pulses k, the transmittance of the glass vial at the respective wavelength T_λ and the desired total photon count n_p.

$$E_0 = \frac{n_p N_A h c}{k T_\lambda \lambda}$$

By controlling the target E_0 at the respective wavelength, the number of photons that penetrates each sample solution of one set of experiments as described in the following subsections was guaranteed to be equal despite irradiation at different wavelengths. Adapted from previous publications.[3–5]

3.7 Transmittance of glass vials used for PLP-experiments

The transmittance of the used glass vials was determined using a method analogue to a previously reported procedure.[3] Glass vials were cut 3 mm above the glass bottom and subjected to an analogous transmittance measurement. Adapted from a previous publication.[3–5]

Figure S7. Cut glass vials for the measurement of the transmittance of the glass bottom. Adapted from a previous publication. [3–5]

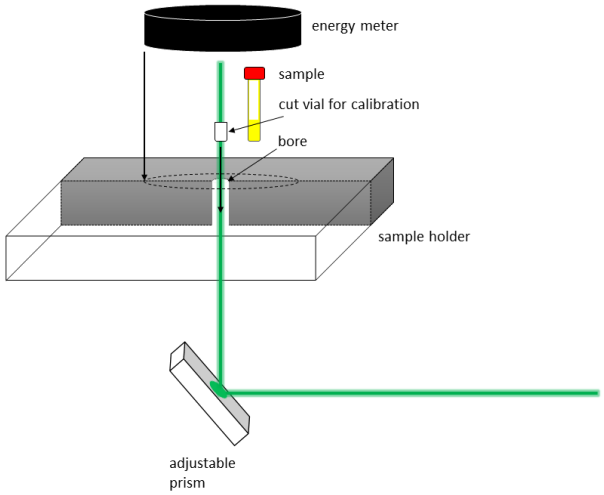

Figure S8. Schematic representation of the setup of the laser experiments and determination of the transmittance of glass vials, which had the headspace section removed, cut 3 mm above the bottom of the glass vial. Adapted from a previous publication.[3–5]

The measurement of the pulse energy of the laser set at a constant energy output was done directly above the sample holder first without a glass vial in the sample holder and subsequently with an empty glass vial in the sample holder. The headspace section of the glass vials and the main part of the glass cylinder was removed for these measurements to detect only the absorbance of the bottom of the vial. The described procedure was performed for five individual glass vials to account for variabilities between the vials. Since the energy of the incident beam on the bottom of the glas vial is most relevant, the following needs to be considered: Light, scattered on the bottom of the glass vial or at the walls of the glass vial might be directed through the sample solution in a laser experiment, while similarly scattered light might not reach the detector above, if the bottom of the glass vial used for the transmittance measurement is located too far away from the detector during this transmittance measurement. Here, the amount of photons in the sample solution with a fill level inside the glass of 10-13 mm is of interest.

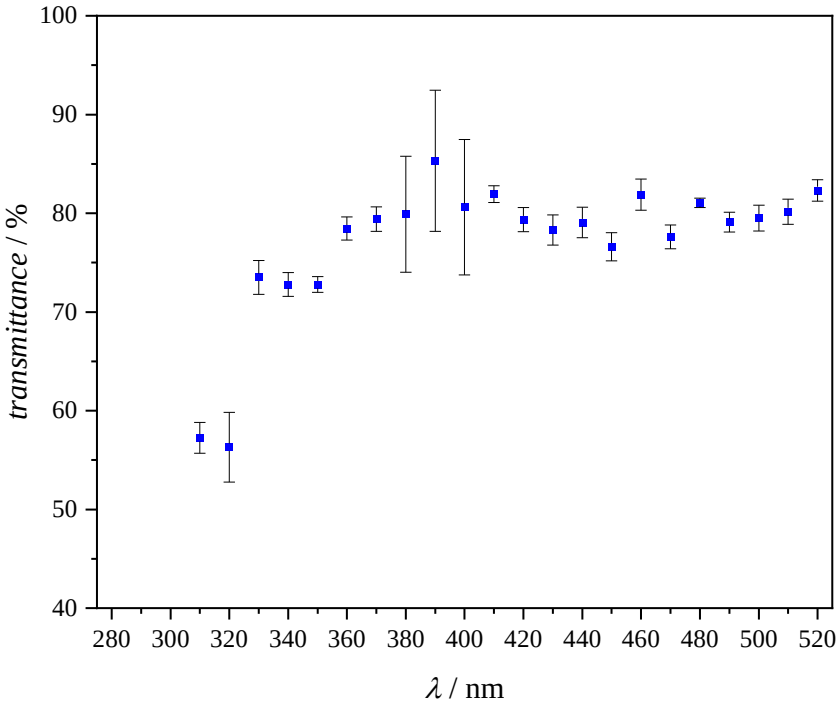

Figure S9. Transmittance of the bottom of glass vials as a function of wavelength.

Table S3. Transmittance of glass vials (bottom and 3 mm wall).

l/nm	Transmittance / %	mean deviation / %
310	57.24	1.56
320	56.30	3.52
330	73.51	1.72
340	72.78	1.19
350	72.78	0.79
360	78.45	1.17
370	79.41	1.25
380	79.89	5.87
390	85.31	7.16
400	80.61	6.86
410	81.94	0.85
420	79.36	1.23
430	78.30	1.54
440	79.06	1.54
450	76.60	1.43
460	81.87	1.58
470	77.60	1.21
480	81.05	0.47
490	79.10	1.01
500	79.51	1.31
510	80.16	1.29
520	82.32	1.09

3.8 Irradiation procedure with control over photon count

The tuneable laser, including the pump source, was started and the internal shutter was opened several minutes before irradiation to allow the energy output of the laser to stabilize. The direction of the beam was controlled by adjusting the orientation of the prism. The entire cross-sectional area of the sample is irradiated by the laser beam. The intensity of the beam was monitored and adjusted with the built-in polarizer (attenuator). A calculated target energy value was set, which enables the irradiation with the desired number of photons during the irradiation time. This general procedure is used for the tunable laser experiments described in the following section. [3–5]

3.9 Sample preparation for laser-experiments

The samples were prepared from a stock solution of ^{Mes}BAPO-NH_2 (c_{PI} = 5.00 mmol L^{-1}) in deinhibited MMA protected from light (yellow light laboratory). 0.3 mL (~ 13 mm layer thickness) aliquots of the stock solution were transferred into crimped 0.7 mL vials by LLG Labware, Lab Logistic Group GmbH (Art. Nr. 4-008202) and degassed by passing through dry nitrogen during 5 minutes with a low flow rate (the loss of MMA during the degassing procedure is below 1.5 %). Afterwards the samples were irradiated according to the information provided in Table S4. After irradiation, the samples were opened to air and the conversion was determined gravimetrically by removal of the unreacted

MMA under high vacuum. Per wavelength three samples were prepared and the average conversion and standard deviation were calculated.

Table S4. Energy per pulse, number of pulses and irradiation time per wavelength and resulting averaged monomer conversion and standard deviation obtained from three samples per wavelength.

λ/nm	Energy E_0 per pulse / mJ	Number of pulses	Irradiation Time / s	Average monomer conversion / %	Std Dev
310	0.749	90000	900	5.24	0.27
320	0.738	90000	900	6.20	0.12
330	0.548	90000	900	6.16	0.48
340	0.537	90000	900	8.15	0.42
350	0.522	90000	900	6.76	0.24
360	0.471	90000	900	6.01	0.67
370	0.452	90000	900	5.68	0.26
380	0.438	90000	900	5.30	0.24
390	0.399	90000	900	5.83	0.38
400	0.412	90000	900	7.08	0.39
410	0.396	90000	900	10.64	0.33
420	0.399	90000	900	12.74	0.48
430	0.395	90000	900	8.20	0.31
440	0.382	90000	900	7.65	0.36
450	0.386	90000	900	9.62	0.13
460	0.353	90000	900	12.35	0.58
470	0.364	90000	900	8.96	0.34
480	0.342	90000	900	1.72	0.15
490	0.343	90000	900	2.37	0.52
500	0.334	90000	900	0.86	0.08
510	0.325	90000	900	0.68	0.09
520	0.311	90000	900	0.42	0.14

4. References

1 O. V. Dolomanov, L. J. Bourhis, R. J. Gildea, J. a. K. Howard and H. Puschmann, *J Appl Cryst*, 2009, **42**, 339–341.

2 G. Müller, M. Zalibera, G. Gescheidt, A. Rosenthal, G. Santiso-Quinones, K. Dietliker and H. Grützmacher, *Macromol. Rapid Commun.*, 2015, **36**, 553–557.

3 D. E. Fast, A. Lauer, J. P. Menzel, A.-M. Kelterer, G. Gescheidt and C. Barner-Kowollik, *Macromol.*, 2017, **50**, 1815–1823.

4 J. P. Menzel, B. B. Noble, A. Lauer, M. L. Coote, J. P. Blinco and C. Barner-Kowollik, *J. Am. Chem. Soc.*, 2017, **139**, 15812–15820.

5 B. T. Tuten, J. P. Menzel, K. Pahnke, J. P. Blinco and C. Barner-Kowollik, *Chem. Commun.*, 2017, **53**, 4501–4504.